WILEY-VCH

Knut and Jakob Stamnes

Radiative Transfer in Coupled Environmental Systems

An Introduction to Forward and Inverse Modeling

Wiley Series in Atmospheric Physics and Remote Sensing

Knut Stamnes and Jakob J. Stamnes

Radiative Transfer in Coupled Environmental Systems

Related Titles

Salam, A.

Molecular Quantum Electrodynamics

Long-Range Intermolecular Interactions

2010
Print ISBN: 978-0-470-25930-6; also available in electronic formats

Ambaum, M.M.

Thermal Physics of the Atmosphere

2010
Print ISBN: 978-0-470-74515-1; also available in electronic formats

Bohren, C.F., Huffman, D.R., Clothiaux, E.E.

Absorption and Scattering of Light by Small Particles

2 Edition

2015
Print ISBN: 978-3-527-40664-7; also available in electronic formats

Wendisch, M., Yang, P.

Theory of Atmospheric Radiative Transfer

A Comprehensive Introduction

2012
Print ISBN: 978-3-527-40836-8; also available in electronic formats

Wendisch, M., Brenguier, J. (eds.)

Airborne Measurements for Environmental Research

Methods and Instruments

2013
Print ISBN: 978-3-527-40996-9; also available in electronic formats

North, G.R., Kim, K.

Energy Balance Climate Models

2013
Print ISBN: 978-3-527-41132-0; also available in electronic formats

Knut Stamnes and Jakob J. Stamnes

Radiative Transfer in Coupled Environmental Systems

An Introduction to Forward and Inverse Modeling

WILEY-VCH
Verlag GmbH & Co. KGaA

Authors

Prof. Knut Stamnes
Stevens Inst. of Technology
Dept. Physics and Eng. Physics
1 Castle Point on Hudson Hoboken
New Jersey 07030
United States

Prof. Jakob J. Stamnes
University of Bergen
Dept. Physics and Technology
P.O. Box 7803
5020 Bergen
Norway

Library of Congress Card No.: applied for

British Library Cataloguing-in-Publication Data
A catalogue record for this book is available from the British Library.

Bibliographic information published by the Deutsche Nationalbibliothek
The Deutsche Nationalbibliothek lists this publication in the Deutsche Nationalbibliografie; detailed bibliographic data are available on the Internet at <http://dnb.d-nb.de>.

Print ISBN: 978-3-527-41138-2
ePDF ISBN: 978-3-527-69662-8
ePub ISBN: 978-3-527-69659-8
Mobi ISBN: 978-3-527-69661-1
oBook ISBN: 978-3-527-69660-4

Cover Design Schulz Grafik-Design, Fußgönheim, Germany
Typesetting SPi Global, Chennai, India
Printing and Binding Markono Print Media Pte Ltd, Singapore

Printed on acid-free paper

Contents

Preface

In a *transparent medium*, it follows from energy conservation that *light attenuation* is proportional to the inverse square of the distance traveled. In a translucent or turbid medium, light suffers attenuation in addition to that given by the *inverse-square law* caused by absorption and scattering, which give an exponential decay in accordance with the *Beer–Lambert law* to a first-order approximation. Application of calculus to interpret experimental results in light attenuation led to the foundation of *radiometry* and the development of appropriate physical theories and mathematical models.

The most important quantity of classical radiative transfer (RT) theory is the *specific intensity* (or *radiance*), defined as the radiant power transported through a surface element in directions confined to a solid angle around the direction of propagation. To treat the *polarization* properties of radiation, Stokes introduced four parameters that describe the state of polarization, which were used by Chandrasekhar to replace the specific intensity with a four-element column vector to describe polarized radiation.

In many applications, an accurate description is required of light propagation in two adjacent slabs of *turbid media* which are separated by an interface, across which the *refractive index* changes. Three important examples of such *coupled media* are atmosphere–water systems, atmosphere–sea ice systems, and air–tissue systems, in which the change in the refractive index across the interface between the two media plays an important role for the transport of light throughout the coupled system. For *imaging* of biological tissues or satellite *remote sensing* of water bodies, an accurate RT model for a coupled system is an indispensable tool. In both cases, an accurate RT tool is essential for obtaining satisfactory solutions of retrieval problems through iterative forward/inverse modeling.

In optical remote sensing of the Earth from space, an important goal is to retrieve atmospheric and surface parameters from measurements of the reflected solar radiation emerging at the top of the atmosphere at a number of wavelengths. These *retrieval parameters*, such as *aerosol type* as well as *loading* and concentrations of aquatic constituents in an open ocean or coastal water area, depend on the *inherent optical properties*, that is, the *scattering* and *absorption* coefficients of the atmosphere and the water. By having a model that provides a

link between retrieval parameters and inherent optical properties, one can use a *forward RT model* to compute how the radiation measured by an instrument deployed on a satellite will respond to changes in the retrieval parameters, and then formulate and solve an *inverse RT problem* to derive information about the retrieval parameters. A forward RT model employing inherent optical properties that describes how atmospheric and aquatic constituents absorb and scatter light can be used to compute the *multiply scattered light field* in any particular direction at any particular depth level in a *vertically stratified medium*, such as a coupled atmosphere–water system. In order to solve an inverse RT problem, it is important to have an accurate and efficient forward RT model. Accuracy is important in order to obtain reliable and robust retrievals, and efficiency is an issue because standard iterative solutions of *nonlinear inverse RT problems* require executing a forward RT model repeatedly to compute the radiation field as well as the partial derivatives with respect to the *retrieval parameters* (the *Jacobians*).

This book is aimed at students with a good undergraduate background in mathematics and physics, but it is kept at a fairly fundamental level. It will teach the reader how to formulate and solve forward and inverse RT problems related to coupled media and gives examples of how to solve concrete problems in remote sensing of coupled atmosphere–surface systems. Thus, it is suitable as a teaching tool for the next generation of environmental scientists and engineers and remote-sensing specialists. It will also be useful for researchers (in academia, industry, and government institutions) in atmospheric and planetary sciences as well as in remote sensing of the environment.

This book discusses RT in coupled media such as the atmosphere–ocean system with *Lambertian* and non-Lambertian reflecting ground surfaces for *polarized* as well as *unpolarized radiation*. The *polarized reflectance* from natural ground surfaces such as plant canopies and wind-roughened water surfaces is discussed, and emphasis is placed on the mathematical description of the *inherent optical properties* of natural media including atmospheric gases and particles, water bodies with embedded impurities (particles), and snow/ice bodies. The spectral range from the *ultraviolet* to the *microwave* region of the electromagnetic spectrum is considered, and *multispectral* and *hyperspectral* remote sensing are discussed, as well as solutions of forward problems for unpolarized and polarized radiation in *coupled media*. A unique feature of this book is that it contains a basic description of inverse methods together with a comprehensive and systematic coverage of formulations and solutions of inverse problems related to coupled media.

Knut Stamnes
Hoboken, New Jersey, USA
June 30, 2015
Jakob J. Stamnes
Bergen, Norway
June 30, 2015

Acknowledgments

Many people have helped us with the creation of this book by contributing to the research behind it, providing feedback on various parts of the text, and helping to create graphic illustrations. We are indebted to several students and colleagues for the contributions, comments, and suggestions, including Nan Chen, Dennis Cohen, Lingling Fan, Yongzhen Fan, Øyvind Frette, Karl I. Gjerstad, Børge Hamre, Min He, Jeff Koskulics, Wei Li, Zhenyi Lin, Jon K. Lotsberg, Matteo Ottaviani, Monika Sikand, Endre R. Sommersten, Snorre Stamnes, and Qiang Tang. We are also grateful to Hilding Lindquist, who helped us in getting the permissions required to use material (illustrations) from published sources. The writing started while KS was on a sabbatical leave from Stevens Institute of Technology. During the period of writing, KS was partially supported by the National Aeronautics and Space Administration (NASA) through a grant from NASA's Remote Sensing Theory Program, a contract from the Japan Aerospace Exploration Agency (JAXA), and a grant from the Air Force Research Laboratory. JJS was partially supported by the Norwegian Research Council.

1
Introduction

1.1
Brief History

The idea or notion that *light attenuation* is proportional to the inverse square of the distance traveled can be traced to Kepler [1]. Its experimental verification was provided by Bouguer [2], who used the inverse square dependence to establish the exponential *extinction law* by studying the attenuation of light passing through *translucent media*. A mathematical foundation of *radiometry* was provided by Lambert [3], who used calculus to interpret experimental results and thereby develop appropriate mathematical models and physical theories. As pointed out by Mishchenko [4], although the first introduction of the *radiative transfer equation (RTE)* has traditionally been attributed to Schuster [5], the credit should go instead to Lommel [6], who derived an integral form of the RTE by considering the directional flow of radiant energy crossing a surface element; almost identical results were obtained independently by Chwolson [7].

The *specific intensity* (or *radiance*) $I(\mathbf{r}, \hat{\mathbf{\Omega}})$ is the most important quantity of classical *radiative transfer theory (RTT)*. Planck [8] defined it by stating that the amount of radiant energy dE transported through a surface element dA in directions confined to a *solid angle* $d\omega$ around the direction of propagation $\hat{\mathbf{\Omega}}$ in a time interval dt is given by $dE = I(\mathbf{r}, \hat{\mathbf{\Omega}}) \cos\theta dA dt d\omega$, where $\mathbf{r}$ is the position vector of the surface element dA, and θ is the angle between $\hat{\mathbf{\Omega}}$ and the normal to dA. This definition was adopted in the works of Milne [9], Hopf [10], and Chandrasekhar [11], and has since been used in many monographs [12–16] and textbooks [17–21] on RTT. To treat the polarization properties of radiation Stokes [22] introduced four parameters to describe the state of polarization. These so-called *Stokes parameters* were used by Chandrasekhar [11, 23] to replace the specific intensity with the four-element column vector $\mathbf{I}(\mathbf{r}, \hat{\mathbf{\Omega}})$ to describe polarized radiation.

The heuristic derivation of the RTE adopted in Chapter 3 of this book for *unpolarized* as well as *polarized radiation* is based on classical RTT invoking the specific intensity and simple energy conservation arguments. Such a derivation is easy to understand and sufficient for our purpose. Mandel and Wolf [24] noted that a more fundamental derivation that can be traced to the *Maxwell equations* was

Radiative Transfer in Coupled Environmental Systems: An Introduction to Forward and Inverse Modeling,
First Edition. Knut Stamnes and Jakob J. Stamnes.

desirable, and stated "In spite of the extensive use of the theory of radiative energy transfer, no satisfactory derivation of its basic equation... from electromagnetic theory... has been obtained up to now." Recently, however, much progress toward such a derivation has been made, as reported by Mishchenko [25].

1.2 What is Meant by a Coupled System?

In many applications, an accurate description is required of light propagation in two adjacent slabs of *turbid media* that are separated by an interface, across which the refractive index changes. Such a two-slab configuration will be referred to as a *coupled system*. Three important examples are atmosphere–water systems [26, 27], atmosphere–sea ice systems [28, 29], and air–tissue systems [30]. In each of these three examples, the change in the refractive index across the interface between the two media must be accounted for in order to model the transport of light throughout the respective coupled system correctly. In the second example, the refractive-index change, together with *multiple scattering*, leads to a significant trapping of light inside the strongly scattering, optically thick sea-ice medium [28, 29]. For *imaging* of biological tissues or satellite remote sensing of water bodies, an accurate radiative transfer (RT) model for a coupled system is an indispensable tool [31, 32]. In both cases, an accurate RT tool is essential for obtaining satisfactory solutions of retrieval problems through iterative forward/inverse modeling [33, 34].

In *remote sensing* of the Earth from space, one goal is to retrieve atmospheric and surface parameters from measurements of the radiation emerging at the top of the atmosphere (TOA) at a number of wavelengths [35, 36]. These *retrieval parameters* (RPs), such as aerosol type and loading and concentrations of aquatic constituents in an open ocean or coastal water area, depend on the *inherent optical properties* (IOPs) of the atmosphere and the water. If there is a model providing a link between the RPs and the IOPs, a forward RT model can be used to compute how the measured TOA radiation field should respond to changes in the RPs, and an inverse RT problem can be formulated and solved to derive information about the RPs [37, 38]. A *forward RT model*, employing IOPs that describe how atmospheric and aquatic constituents absorb and scatter light can be used to compute the *multiply scattered light field* in any particular direction (with specified polar and azimuth angles) at any particular depth level (including the TOA) in a vertically *stratified medium*, such as a coupled atmosphere–water system [34, 39]. In order to solve the *inverse RT problem*, it is important to have an accurate and efficient forward RT model. Accuracy is important in order to obtain reliable and robust retrievals, and efficiency is an issue because standard iterative solutions of the *nonlinear inverse RT problem* require executing the forward RT model repeatedly to compute the radiation field and its partial derivatives with respect to the RPs (the *Jacobians*) [37, 38].

1.3 Scope

While solutions to the *scalar RTE*, which involve only the first component of the *Stokes vector* (the radiance or intensity), are well developed, modern RT models that solve the *vector RTE* are capable of also accounting for polarization effects described by the second, third, and fourth components of the Stokes vector. Even if one's interest lies primarily in the radiance, it is important to realize that solutions of the *scalar RTE*, which ignores *polarization effects*, introduce errors in the computed radiances [40–42].

In this book, we will consider the theory and applications based on both scalar and vector RT models, which include polarization effects. There are numerous RT models available that include polarization effects (see Zhai *et al.* [43] and references therein for a list of papers), and the interest in applications based on *polarized radiation* is growing. There is also a growing interest in applications based on vector RT models that apply to coupled systems. Examples of vector RT modeling pertinent to a coupled atmosphere–water system include applications based on the *doubling-adding method* (e.g., Chowdhary [44], Chowdhary *et al.*, [45–47]), the *successive order of scattering method* (e.g., Chami *et al.*, [48], Min and Duan [49], Zhai *et al.*, [43]), the *matrix operator method* (e.g., Fisher and Grassl, [50], Ota *et al.*, [51]), and *Monte Carlo methods* (e.g., Kattawar and Adams [40], Lotsberg and Stamnes [52]).

Chapter 2 provides definitions of IOPs including *absorption* and *scattering coefficients* as well as the *normalized angular scattering cross section*, commonly referred to as the *scattering phase function*, and the corresponding *scattering phase matrix* needed for vector RT modeling and applications. In several subsections basic scattering theory with emphasis on spherical particles (*Mie–Lorenz theory*) is reviewed, and IOPs for atmospheric gases and aerosols as well those for surface materials including snow/ice, liquid water, and land surfaces are discussed. The impact of a rough interface between the two adjacent slabs is also discussed.

In Chapter 3, an overview is given of the *scalar RTE* as well as the *vector RTE* applicable to a coupled system consisting of two adjacent slabs with different refractive indices. Several methods of solution are discussed: the *successive order of scattering method*, the *discrete-ordinate method*, the *doubling-adding method*, and the *Monte Carlo method*. In Chapter 4, we discuss forward RT modeling in coupled environmental systems based on the discrete-ordinate method, while Chapter 5 is devoted to a discussion of the inverse problem. Finally, in Chapter 6, a few typical applications are discussed including (i) how spectral redundancy can be exploited to reduce the computational burden in atmospheric RT problems, (ii) simultaneous retrieval of total ozone column amount and cloud effects from ground-based irradiance measurements, (iii) retrieval of aerosol and snow-ice properties in coupled atmosphere–cryosphere systems from space, (iv) retrieval of aerosol and aquatic parameters in coupled atmosphere–water systems from space, (v) vector RT in coupled systems, and (vi) how polarization measurements

can be used to improve retrievals of atmospheric and surface parameters in coupled atmosphere–surface systems.

1.4 Limitations of Scope

We restrict our attention to scattering by molecules and small particles such as aerosols and cloud particles in an atmosphere, hydrosols in water bodies such as oceans, lakes, and rivers, and inclusions (air bubbles and brine pockets) embedded in ice. To explain the meaning of *independent scattering*, let us consider an infinitesimal volume element filled with small particles that are assumed to be randomly distributed within the volume element. Such infinitesimal volume elements are assumed to constitute the elementary scattering agents. *Independent scattering* implies that each particle in each of the infinitesimal volume elements is assumed to scatter radiation independently of all other volume elements.

Although there are many applications that require a three-dimensional (3-D) RT treatment, in this book we limit our discussion to *plane-parallel* systems with an emphasis on the coupling between the atmosphere and the underlying surface consisting of a water body, a snow/ice surface, or a vegetation canopy. For a clear (cloud- and aerosol-free) atmosphere, 3-D effects are related to the impact of the Earth's curvature on the radiation field. To include such effects, a *pseudo-spherical* treatment (see Dahlback and Stamnes [53]) may be sufficient, in which the direct solar beam illumination is treated using spherical geometry, whereas *multiple scattering* is done using a plane-parallel geometry. This pseudo-spherical approach has been implemented in many RT codes [54, 55]. There is a large body of literature on *3-D RT modeling* with applications to broken clouds. Readers interested in RT in cloudy atmospheres may want to consult books like that of Marshak and Davis [12] or visit the Web site http://i3rc.gsfc.nasa.gov/.

3-D RT modeling may also be important for analysis and interpretation of *lidar* data. In this context, the classical "searchlight problem" [56], which considers the propagation of a *laser beam* through a *turbid medium*, is relevant. Long-range propagation of a lidar beam has been studied both theoretically and experimentally [57]. Monte Carlo simulations are well suited for such studies [58], and use of deterministic models such the *discrete-ordinate method*, discussed in Chapters 3 and 4 of this book, have also been reported [59, 60].

Most RT studies in the ocean have been concerned with understanding the propagation of sunlight, as discussed by Mobley *et al.* [26]. For these applications, the transient or *time-dependent* term in the RTE can be ignored, because changes in the incident illumination are much slower than the changes imposed by the propagation of the light field through the medium. While this assumption is satisfied for solar illumination, lidar systems can use pulses that are shorter than the attenuation distance of seawater divided by the speed of light in water. Also, as

pointed out by Mitra and Churnside [61], due to multiple light scattering, understanding the lidar signal requires a solution of the *time-dependent RTE*. Although such studies are beyond the scope of this book, the transient RT problem can be reduced to solving a series of *time-independent* RT problems, as discussed by Stamnes *et al.* [62].

We restrict our attention to *elastic scattering*, although *inelastic scattering* processes (Raman and Brillouin) certainly can be very important and indeed essential in some atmospheric [63–65] and aquatic [66, 67] applications. Although most particles encountered in nature have nonspherical shapes – cloud droplets being the notable exception – we will not consider nonspherical particles in this book. Although the general introduction to the scattering problem provided in Chapter 2 is generic in nature and thus applies to particles of arbitrary shape, our more detailed review is limited to spherical particles (Mie–Lorenz theory). The reader is referred to the books by Bohren and Huffman [68] and Zdunkowski *et al.* [20] for a more comprehensive discussion of the Mie-Lorenz theory and to the recent book by Wendisch and Yang [21] for an excellent introduction to scattering by nonspherical particles.

2
Inherent Optical Properties (IOPs)

2.1
General Definitions

2.1.1
Absorption Coefficient and Volume Scattering Function

The optical properties of a medium can be categorized as inherent or apparent. An *inherent optical property* (IOP) depends only on the medium itself, and not on the ambient light field within the medium [69]. An *apparent optical property* (AOP) depends also on the illumination, and hence on light propagating in particular directions inside and outside the medium[1)].

The *absorption coefficient* α and the *scattering coefficient* β are important IOPs, defined as [18]

$$\alpha(s) = \frac{1}{I^i}\left(\frac{dI^\alpha}{ds}\right) \tag{1}$$

$$\beta(s) = \frac{1}{I^i}\left(\frac{dI^\beta}{ds}\right). \tag{2}$$

Here, I^i is the *radiance* of the incident light beam entering a volume element $dV = dA\,ds$ of the medium of cross-sectional area dA and length ds, and $dI^\alpha > 0$ and $dI^\beta > 0$ are, respectively, the radiances that are absorbed and scattered in all directions as the light beam propagates the distance ds, which is the thickness of the volume element dV along the direction of the incident light beam. If the distance ds is measured in meters, the unit for the absorption or scattering coefficient defined in Eq. (1) or Eq. (2) becomes [m^{-1}]. The *extinction coefficient* γ is the sum of the absorption and scattering coefficients

$$\gamma(s) = \alpha(s) + \beta(s) \tag{3}$$

1) Apparent optical properties (i) depend both on the medium (the IOPs) and on the geometric (directional) structure of the radiance distribution, and (ii) display enough regular features and stability to be useful descriptors of a water body [69]. Hence, a radiance or an irradiance would satisfy only the first part of the definition, while a radiance or irradiance reflectance, obtained by division of the radiance or the upward irradiance by the downward irradiance, would satisfy also the second part of the definition.

Radiative Transfer in Coupled Environmental Systems: An Introduction to Forward and Inverse Modeling,
First Edition. Knut Stamnes and Jakob J. Stamnes.

and the *single-scattering albedo* ϖ is defined as the ratio of β to γ

$$\varpi(s) = \frac{\beta(s)}{\gamma(s)}. \tag{4}$$

Thus, given an interaction between an incident light beam and the medium, the single-scattering albedo, which varies between 0 and 1, gives the probability that the light beam will be scattered rather than absorbed.

The angular distribution of the scattered light is given in terms of the *volume scattering function* (vsf), which is defined as

$$\mathrm{vsf}(s, \hat{\mathbf{\Omega}}', \hat{\mathbf{\Omega}}) = \frac{1}{I^i}\frac{d^2 I^\beta}{ds\, d\omega} = \frac{1}{I^i}\frac{d}{ds}\left(\frac{dI^\beta}{d\omega}\right) \quad [\mathrm{m}^{-1}\mathrm{sr}^{-1}]. \tag{5}$$

Here, $d^2 I^\beta$ is the *radiance* scattered from an incident direction $\hat{\mathbf{\Omega}}'$ into a cone of solid angle $d\omega$ around the direction $\hat{\mathbf{\Omega}}$ as the light propagates the distance ds along $\hat{\mathbf{\Omega}}'$. The plane spanned by the unit vectors $\hat{\mathbf{\Omega}}'$ and $\hat{\mathbf{\Omega}}$ is called the *scattering plane*, and the *scattering angle* Θ is given by $\cos\Theta = \hat{\mathbf{\Omega}}' \cdot \hat{\mathbf{\Omega}}$. Integration on the far right side of Eq. (5) over all scattering directions yields, using Eq. (2)

$$\begin{aligned}\beta(s) &= \frac{1}{I^i}\frac{d}{ds}\int_{4\pi}\left(\frac{dI^\beta}{d\omega}\right)d\omega = \frac{1}{I^i}\left(\frac{dI^\beta}{ds}\right) \\ &= \int_{4\pi}\mathrm{vsf}(s, \hat{\mathbf{\Omega}}', \hat{\mathbf{\Omega}})d\omega = \int_0^{2\pi}\int_0^{\pi}\mathrm{vsf}(s, \cos\Theta, \phi)\sin\Theta d\Theta d\phi\end{aligned} \tag{6}$$

where Θ and ϕ are, respectively, the polar angle and the azimuth angle in a spherical coordinate system, in which the polar axis is along $\hat{\mathbf{\Omega}}'$. As indicated in Eq. (6), the vsf is generally a function of both Θ and ϕ, but for randomly oriented scatterers one may assume that the scattering potential is spherically symmetric, implying that there is no azimuthal dependence, so that $\mathrm{vsf} = \mathrm{vsf}(s, \cos\Theta)$. Then one finds, with $x = \cos\Theta$

$$\beta(s) = 2\pi\int_0^{\pi}\mathrm{vsf}(s, \cos\Theta)\sin\Theta d\Theta = 2\pi\int_{-1}^{1}\mathrm{vsf}(s, x)dx. \tag{7}$$

2.1.2 Scattering Phase Function

A normalized *vsf*, denoted by $p(s, \cos\Theta)$ and referred to hereafter as the *scattering phase function*, may be defined as follows:

$$p(s, \cos\Theta) = 4\pi\frac{\mathrm{vsf}(s, \cos\Theta)}{\int_{4\pi}\mathrm{vsf}(s, \cos\Theta)d\omega} = \frac{\mathrm{vsf}(s, \cos\Theta)}{\frac{1}{2}\int_{-1}^{1}\mathrm{vsf}(s, x)dx} \tag{8}$$

so that

$$\frac{1}{4\pi}\int_{4\pi}p(s, \cos\Theta)d\omega = \frac{1}{2}\int_{-1}^{1}p(s, x)dx = 1. \tag{9}$$

The scattering phase function has the following physical interpretation: Given that a scattering event has occurred, $p(s, \cos\Theta)d\omega/4\pi$ is the probability that a light

beam traveling in the direction $\hat{\mathbf{\Omega}}'$ is scattered into a cone of solid angle $d\omega$ around the direction $\hat{\mathbf{\Omega}}$ within the volume element dV with thickness ds along $\hat{\mathbf{\Omega}}'$.

The scattering phase function $p(s, \cos\Theta)$ describes the angular distribution of the scattering, while the scattering coefficient $\beta(s)$ describes its magnitude. A convenient measure of the "shape" of the scattering phase function is the average over all scattering directions (weighted by $p(s, \cos\Theta)$) of the cosine of the scattering angle Θ, that is,

$$g(s) = \langle \cos\Theta \rangle = \frac{1}{4\pi} \int_{4\pi} p(s, \cos\Theta)\ \cos\Theta\, d\omega$$
$$= \frac{1}{2} \int_0^{\pi} p(s, \cos\Theta)\ \cos\Theta\ \sin\Theta\, d\Theta = \frac{1}{2} \int_{-1}^{1} p(s, x)\, x\, dx \tag{10}$$

where $x = \cos\Theta$. The average cosine $g(s)$ is called the *asymmetry factor* of the scattering phase function. Equation (10) yields complete forward scattering if $g = 1$ and complete backward scattering if $g = -1$, and $g = 0$ if $p(s, \cos\Theta)$ is symmetric about $\Theta = 90°$. Thus, *isotropic scattering* also gives $g = 0$. The *scattering phase function* $p(s, \cos\Theta)$ depends on the *refractive index* as well as the size of the scattering particles, and will thus depend on the physical situation and the practical application of interest. The probability of scattering into the backward hemisphere is given by the *backscattering ratio* (or *backscatter fraction*) b, defined as

$$b(s) = \frac{1}{2} \int_{\pi/2}^{\pi} p(s, \cos\Theta)\ \sin\Theta\, d\Theta = \frac{1}{2} \int_0^{1} p(s, -x)\, dx. \tag{11}$$

The scattering phase function may be approximated by a finite sum of $(M + 1)$ Legendre polynomials (dropping for simplicity the dependence on the position s)

$$p(\cos\Theta) \approx \sum_{\ell=0}^{M} (2\ell + 1)\chi_\ell P_\ell(\cos\Theta) \tag{12}$$

where P_ℓ is the ℓth *Legendre polynomial*, and the *expansion coefficient* is given by

$$\chi_\ell = \frac{1}{2} \int_{-1}^{1} P_\ell(x) p(x) dx. \tag{13}$$

The Legendre polynomials satisfy an orthogonality relation

$$\frac{1}{2} \int_{-1}^{+1} P_\ell(x) P_k(x) dx = \frac{1}{2\ell + 1} \delta_{\ell k} \tag{14}$$

as well as an *Addition Theorem*:

$$P_\ell(\cos\Theta) = P_\ell(u') P_\ell(u) + 2 \sum_{m=1}^{\ell} \Lambda_\ell^m(u') \Lambda_\ell^m(u) \cos m(\phi' - \phi) \tag{15}$$

where $u = \cos\theta$, $u' = \cos\theta'$,

$$\Lambda_\ell^m(u) = \sqrt{\frac{(\ell - m)!}{(\ell + m)!}} P_\ell^m(u)$$

and $P_\ell^m(u)$ is the *associated Legendre polynomial*. For $m = 0$, we have $\Lambda_\ell^0(u) = P_\ell^0(u) = P_\ell(u)$. The scattering angle Θ is related to the polar and azimuthal angles by

$$\cos\Theta = uu' + \sqrt{1-u^2}\sqrt{1-u'^2}\cos(\phi' - \phi) \tag{16}$$

where (θ', ϕ') and (θ, ϕ) are the polar and azimuthal angles before and after scattering, respectively. Substituting Eq. (15) into Eq. (12), we have

$$p(\cos\Theta) = p(u', \phi'; u, \phi) \approx \sum_{\ell=0}^{M} (2\ell+1)\chi_\ell \times \left\{ P_\ell(u')P_\ell(u) + 2\sum_{m=1}^{\ell} \Lambda_\ell^m(u')\Lambda_\ell^m(u)\cos m(\phi' - \phi) \right\} \tag{17}$$

which can be rewritten as a *Fourier cosine series*

$$p(u', \phi'; u, \phi) \approx \sum_{m=0}^{M} (2 - \delta_{m0})\, p^m(u', u)\cos m(\phi' - \phi) \tag{18}$$

where δ_{0m} is the Kronecker delta, that is, $\delta_{0m} = 1$ for $m = 0$ and $\delta_{0m} = 0$ for $m \neq 0$, and

$$p^m(u', u) \approx \sum_{\ell=m}^{M} (2\ell+1)\chi_\ell \Lambda_\ell^m(u')\Lambda_\ell^m(u). \tag{19}$$

In a *plane-parallel* or *slab geometry*, *irradiances* and the *scalar radiance* (*mean intensity*) depend on the azimuthally averaged phase function. Application of azimuthal averaging, that is, $\frac{1}{2\pi}\int_0^{2\pi} d\phi \cdots$, to both sides of Eq. (12), combined with Eq. (15) or Eq. (18) gives

$$p(u', u) \equiv p^0(u', u) = \frac{1}{2\pi}\int_0^{2\pi} p(u', \phi'; u, \phi)d\phi \approx \sum_{\ell=0}^{M} (2\ell+1)\chi_\ell P_\ell(u)P_\ell(u'). \tag{20}$$

From Eq. (20), it follows that

$$\frac{1}{2}\int_{-1}^{1} p(u', u)P_k(u')du' \approx \sum_{\ell=0}^{M} (2\ell+1)\chi_\ell P_\ell(u)\frac{1}{2}\int_{-1}^{1} P_\ell(u')P_k(u')du' \tag{21}$$

which by the use of orthogonality [Eq. (14)] leads to

$$\chi_\ell = \frac{1}{P_\ell(u)}\,\frac{1}{2}\int_{-1}^{1} p(u', u)P_\ell(u')du'. \tag{22}$$

Thus, to calculate the *expansion coefficients* or *moments* χ_ℓ, we can use the azimuthally averaged phase function $p(u', u)$ given by Eq. (20).

Four different scattering phase functions, which are useful in practical applications, are discussed below.

2.2
Examples of Scattering Phase Functions

2.2.1
Rayleigh Scattering Phase Function

When the size d of a scatterer is small compared to the wavelength of light ($d < \frac{1}{10}\lambda$), the *Rayleigh scattering phase function* gives a good description of the angular distribution of the scattered light. It is given by [see Eq. (59)]

$$p_{\text{Ray}}(\cos\Theta) = \frac{3}{3+f}(1 + f\cos^2\Theta) \tag{23}$$

where the parameter $f = \frac{1-\rho}{1+\rho}$, and ρ is the *depolarization factor* defined in Eq. (63), attributed to the anisotropy of the scatterer (the molecule) [70–73]. Originally, this *scattering phase function* was derived for light scattering by an electric dipole [74]. Since the Rayleigh scattering phase function is symmetric about $\Theta = 90°$, the *asymmetry factor* is $g = \chi_1 = 0$. If the Rayleigh scattering phase function is expanded in *Legendre polynomials*, the *expansion coefficients* χ_ℓ [see Eqs. (13) and (22)] are simply given by $\chi_0 = 1$, $\chi_1 = 0$, $\chi_2 = \frac{2f}{5(3+f)}$, and $\chi_\ell = 0$ for $\ell > 2$ (see Problem 2.1). For Rayleigh scattering, a value of $\rho = 0.04$ for air gives $f_{\text{air}} = 0.923$, while for water the numerical value $\rho = 0.09$ is commonly used, implying $f_{\text{water}} = 0.835$. For inelastic *Raman scattering*, the scattering phase function is the same as for Rayleigh scattering except that $\rho = 0.29$, implying $f_{\text{water}}^{\text{Raman}} = 0.55$.

2.2.2
Henyey–Greenstein Scattering Phase Function

In 1941, Henyey and Greenstein [75] proposed a one-parameter scattering phase function given by (suppressing the dependence on the position s)

$$p_{\text{HG}}(\cos\Theta) = \frac{1-g^2}{(1+g^2-2g\cos\Theta)^{3/2}} \tag{24}$$

where the parameter g is the asymmetry factor defined in Eq. (10). The *Henyey–Greenstein (HG) scattering phase function* has no physical basis, but is very useful for describing a highly scattering medium, such as turbid water or sea ice, for which the actual scattering phase function is unknown. The HG scattering phase function is convenient for Monte Carlo simulations and other numerical calculations because of its analytical form. In deterministic plane-parallel RT models, it is also very convenient because the *addition theorem* of spherical harmonics can be used to expand the scattering phase function in a series of Legendre polynomials [18], as reviewed in the previous section. For the HG scattering phase function, the expansion coefficients χ_ℓ in this series [see Eqs. (13) and (22)] are simply given by $\chi_\ell = g^\ell$, implying that the HG scattering phase function can be approximated

by a finite sum of $(M + 1)$ Legendre polynomials [see Eq. (12) and Problem 2.2)]

$$p_{\mathrm{HG}}(\cos\Theta) = \frac{1-g^2}{(1+g^2-2g\,\cos\,\Theta)^{3/2}} \approx \sum_{\ell=0}^{M}(2\ell+1)g^{\ell}P_{\ell}(\cos\Theta). \tag{25}$$

The HG scattering phase function is useful for scatterers with sizes comparable to or larger than the wavelength of light.

The probability of scattering into the backward hemisphere, the *backscattering ratio* (or backscatter fraction) becomes [see Eq. (11)]:

$$\begin{aligned} b_{\mathrm{HG}} &= \frac{1}{2}\int_0^1 p(s,-x)\,dx = \frac{1-g^2}{2}\int_0^1 \frac{dx}{(1+g^2+2g\,x)^{3/2}} \\ &= \frac{1-g}{2g}\left[\frac{(1+g)}{\sqrt{(1+g^2)}}-1\right]. \end{aligned} \tag{26}$$

Figure 1 shows the scattering phase functions computed for a collection of particles with a log-normal size distribution (see Section 2.4.3 and Eq. (102)). The left panel pertains to nonabsorbing aerosol particles with *refractive index* $n = 1.385$, mode radius $r_n = 0.3$ μm, and standard deviation $\sigma_n = 0.92$, and the smallest and largest radii are selected to be $r_1 = 0.005$ μm and $r_2 = 30$ μm. The right panel pertains to nonabsorbing cloud droplets with refractive index $n = 1.339$, mode radius $r_n = 5$ μm, and standard deviation $\sigma_n = 0.4$, and the smallest and largest radii are selected to be $r_1 = 0.005$ μm and $r_2 = 100$ μm.

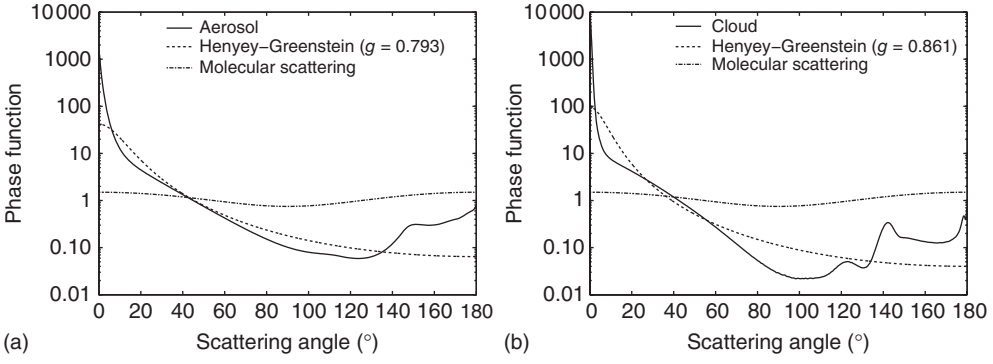

Figure 1 Scattering phase functions calculated using a Mie code. (a) For aerosols with asymmetry factor 0.79275. (b) For clouds with asymmetry factor 0.86114. HG scattering phase functions [see Eq. (24)] with asymmetry factors equal to those for the cloud and aerosol particles are shown for comparison. The Rayleigh scattering phase function [Eq (23)] describing molecular scattering is also shown for comparison.

2.2.3 Fournier–Forand Scattering Phase Function

Measurements have shown that the *particle size distribution* (PSD) in oceanic water can be accurately described by a power law (*Junge distribution*) $n(r) = C(\xi, r_1, r_2)/r^{\xi}$, where $n(r)$ is the number of particles per unit volume per unit bin width, r [μm] is the radius of the assumed spherical particles, and r_1 and r_2 denote the smallest and largest particle size, respectively. The normalization constant $C(\xi, r_1, r_2)$ [$\mathrm{cm}^{-3} \cdot \mu\mathrm{m}^{\xi-1}$] is called the *Junge coefficient*, and $\xi > 0$ is the PSD slope, which typically varies between 3.0 and 5.0 (Diehl and Haardt [76]; McCave [77]). The power-law PSD is further described in Section 2.4.3. By assuming a power law for the PSD, and letting each particle scatter in accordance with the anomalous diffraction approximation, Fournier and Forand [78] derived an analytic expression for the scattering phase function of oceanic water (hereafter referred to as the FF scattering phase function). A commonly used version of the *FF scattering phase function* is given by (Mobley *et al.*, [79])

$$p_{\mathrm{FF}}(\Theta) = \frac{1}{4\pi(1-\delta)^2\delta^{\nu}}\left\{\nu(1-\delta) - (1-\delta^{\nu}) + \frac{4}{\tilde{u}^2}[\delta(1-\delta^{\nu}) - \nu(1-\delta)]\right\} + \frac{1-\delta_{180}^{\nu}}{16\pi(\delta_{180}-1)\delta_{180}^{\nu}}[3\cos^2\Theta - 1] \tag{27}$$

where $\nu = 0.5(3-\xi)$,

$$\delta \equiv \delta(\Theta) = \frac{\tilde{u}^2(\Theta)}{3(n-1)^2}$$

$\tilde{u}(\Theta) = 2\sin(\Theta/2)$, $\delta_{180} = \delta(\Theta = 180^{\circ}) = \frac{4}{3(n-1)^2}$, Θ is the *scattering angle*, and n is the real part of the *refractive index*. Note that, in addition to the scattering angle Θ, the *FF scattering phase function* depends also on the real part of the refractive index of the particle relative to water and the *slope parameter* ξ characterizing the PSD.

Setting $x = -\cos\Theta$, and integrating the FF scattering phase function over the backward hemisphere, one obtains the *backscattering ratio* or *backscatter fraction* defined in Eq. (11), that is, [79]

$$b_{\mathrm{FF}} = \frac{1}{2}\int_{\pi/2}^{\pi} p_{\mathrm{FF}}(\cos\Theta)\sin\Theta d\Theta = \frac{1}{2}\int_0^1 p_{\mathrm{FF}}(-x)\,dx = 1 - \frac{1-\delta_{90}^{\nu+1} - 0.5(1-\delta_{90}^{\nu})}{(1-\delta_{90})\delta_{90}^{\nu}} \tag{28}$$

where $\delta_{90} = \delta(\Theta = 90^{\circ}) = \frac{4}{3(n-1)^2}\sin^2(45^{\circ}) = \frac{2}{3(n-1)^2}$. Equation (28) can be solved for ν in terms of b_{FF} and δ_{90}, implying that ν and thus ξ can be determined if the real part of the refractive index n and the *backscattering ratio* b_{FF} are specified. As a consequence, the FF scattering phase function can be evaluated from the measured value of b_{FF} if the real part of the refractive index n is known.

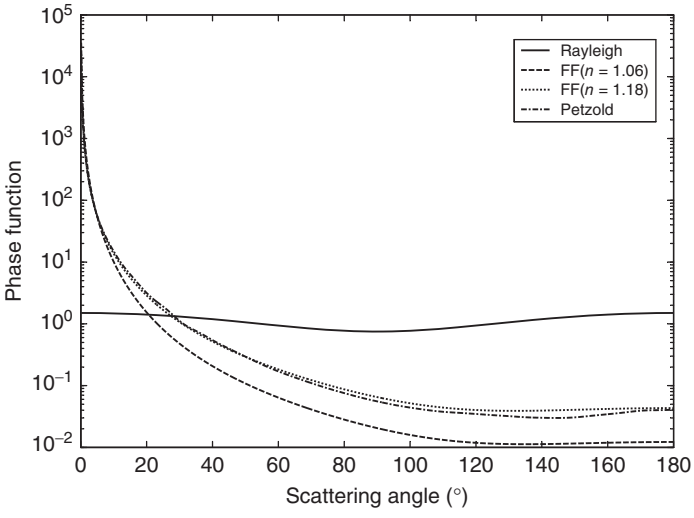

Figure 2 Rayleigh [Eq. (23)], FF [Eq. (27)], and Petzold scattering phase functions.

2.2.4
The Petzold Scattering Phase Function

The vsfs measured by Petzold [80] have been widely used by ocean optics researchers. These *scattering phase functions* are discussed by Mobley [69], who tabulated the vsfs for clear ocean, coastal ocean, and turbid harbor waters. Based on these three vsfs, an average scattering phase function for supposedly "typical" ocean waters was created (Mobley *et al.* [26], Table 2). This average *Petzold scattering phase function*, which has an asymmetry factor $g = 0.9223$ and a backscattering ratio $b_{\mathrm{FF}} = 0.019$, is shown in Figure 2 together with the *Rayleigh scattering phase function* and the *FF scattering phase function*. For the FF phase function, the power-law slope was set to $\xi = 3.38$, but results for two different values of the real part of the refractive index are shown: $n = 1.06$ and $n = 1.18$. These values yield an asymmetry factor $g = 0.9693$ and a backscattering ratio $b_{\mathrm{FF}} = 0.0067$ for $n = 1.06$ and $g = 0.9160$ and $b_{\mathrm{FF}} = 0.022$ for $n = 1.18$. Note the similarity between the FF scattering phase function for $n = 1.18$ and the average Petzold scattering phase function, which indicates that the average Petzold scattering phase function is more suitable for mineral-dominated waters than for pigment-dominated waters.

2.3
Scattering Phase Matrix

The theoretical development of *vector radiative transfer theory* starts with the *Stokes vector* representation $\mathbf{I} = [I_{\|}, I_{\perp}, U, V]^T$, where the superscript T denotes